Food Packaging and Shelf Life 17 (2018) 39–49

Contents lists available at ScienceDirect

Food Packaging and Shelf Life

journal homepage: www.elsevier.com/locate/fpsl

Melt processability, characterization, and antibacterial activity of compression-molded green composite sheets made of poly(3-hydroxybutyrate-*co*-3-hydroxyvalerate) reinforced with coconut fibers impregnated with oregano essential oil

S. Torres-Giner[a,*], L. Hilliou[b], B. Melendez-Rodriguez[a], K.J. Figueroa-Lopez[a], D. Madalena[c], L. Cabedo[d], J.A. Covas[b], A.A. Vicente[c], J.M. Lagaron[a]

[a] Novel Materials and Nanotechnology Group, Institute of Agrochemistry and Food Technology (IATA), Spanish Council for Scientific Research (CSIC), Paterna, Spain
[b] Institute for Polymers and Composites/I3N, University of Minho, Guimarães, Portugal
[c] CEB - Centre of Biological Engineering, University of Minho, Braga, Portugal
[d] Polymers and Advanced Materials Group (PIMA), Universitat Jaume I (UJI), Castellón, Spain

ARTICLE INFO

Keywords:
PHBV
Coir
Essential oils
Active packaging
Agro-food waste valorization

ABSTRACT

New packaging materials based on green composite sheets consisting of poly(3-hydroxybutyrate-*co*-3-hydroxyvalerate) (PHBV) and coconut fibers (CFs) were obtained by twin-screw extrusion (TSE) followed by compression molding. The effect of varying the CF weight content, *i.e.* 1, 3, 5, and 10 wt.-%, and the screw speed during melt processing, *i.e.* 75, 150, and 225 rpm, on both the aspect ratio and dispersion of the fibers was analyzed and related to the properties of the compression-molded sheets. Finally, the CFs were impregnated with oregano essential oil (OEO) by an innovative spray coating methodology and then incorporated into PHBV at the optimal processing conditions. The functionalized green composite sheets presented bacteriostatic effect against *Staphylococcus aureus* from fiber contents as low as 3 wt.-%. Therefore, the here-prepared CFs can be successfully applied as natural vehicles to entrap extracts and develop green composites of high interest in active food packaging to provide protection and shelf life extension.

1. Introduction

The use of agro-food residues for the preparation of polymer composites is gaining a significant attention due to their huge availability and low price, being at the same time a highly sustainable strategy for waste valorization. Natural fibers (NFs), particularly those obtained from plants, represent an environmentally friendly and unique choice to reinforce bioplastic matrices due to their relative high strength and stiffness (Yang, Kim, Park, Lee, & Hwang, 2006). The substitution of oil-derived polymers with bio-based polymers as the matrix component results in the term “green composites” (Zini & Scandola, 2011), which indicates that the composite as a whole, *i.e.* both matrix and reinforcement, originates from renewable resources. In this regard, the incorporation of NFs such as jute, sisal, flax, hemp, and bamboo fibers into biopolymers has been recently intensified (Bogoeva-Gaceva et al., 2007). Resultant green composites do not only offer environmental advantages over traditional polymer composites, such as reduced dependence on non-renewable energy/material sources, lower greenhouse gas and pollutant emissions, improved energy recovery, and end-of-life biodegradability of components (Joshi, Drzal, Mohanty, & Arora, 2004), but also a potential reduction of both product density and energy requirements for processing (Faruk, Bledzki, Fink, & Sain, 2014).

Polyhydroxyalkanoates (PHAs) comprise a family of biodegradable aliphatic polyesters produced by microorganisms. PHAs show the highest potential to replace polyolefins in a wide range of applications, including packaging, due to their high mechanical strength and water resistance (Bugnicourt, Cinelli, Lazzeri, & Alvarez, 2014). Among PHAs, poly(3-hydroxybutyrate) (PHB) and its copolymer with 3-hydroxyvalerate (HV), *i.e.* poly(3-hydroxybutyrate-*co*-3-hydroxyvalerate) (PHBV), have so far received the greatest attention in terms of pathway characterization and industrial-scale production. The use of PHA copolymers presents certain advantages since they have a lower melting point and higher flexibility than their homopolymers, which improves melt stability and broadens their processing window (Torres-Giner, Montanes, Boronat, Quiles-Carrillo, & Balart, 2016). Furthermore, the

* Corresponding author.
E-mail address: storresginer@iata.csic.es (S. Torres-Giner).

https://doi.org/10.1016/j.fpsl.2018.05.002
Received 30 December 2017; Received in revised form 29 March 2018; Accepted 2 May 2018

introduction of comonomer units induces defects in the crystal lattice, reducing both the degree of crystallinity and crystallization rate (Kunioka, Tamaki, & Doi, 1989).

Several plant-derived NFs, such as regenerated and/or recycled cellulose, pineapple leaf fibers (PALF), wheat straw fibers, wood floor, jute fibers, flax fibers, banana, sisal, and coir fibers, hemp fibers, abaca fibers, bamboo fibers, sugarcane bagasse fibers, kenaf and lyocell fibers, wood powder, and pita (agave) fibers, have been so far studied as sustainable reinforcements to produce PHA-based composite materials (Torres-Giner, Montanes, Fombuena, Boronat, & Sanchez-Nacher, 2016). Recently, cellulose fibers from wheat straw and other by-products have been used in the European Projects ECOBIOCAP and YPACK as a cheap source of fillers to reduce the cost of a PHA matrix for packaging applications, where up to 20% of cellulose fibers were allowed in the final composition. Some previous research studies have also suggested that the incorporation of NFs can definitely strengthen the mechanical performance of both PHB and PHBV and, in some cases, also improve biodegradability (Avella et al., 2000; Barkoula, Garkhail, & Peijs, 2010; Teramoto, Urata, Ozawa, & Shibata, 2004). However, the narrow processing window and the poor melt strength of PHAs are certainly responsible for the rather small number of studies involving extruded composites with potential for being converted into packaging articles such as films and sheets (Cunha et al., 2015). The most promising PHA-based composite manufacturing techniques are extrusion and compression molding, particularly the latter, given the relatively low shear-rates and thermomechanical stresses involved.

Coconut shells represent a good example of agro-industrial non-food feedstock that is still considered as waste, for which relevant industrial new end uses are being currently pursued (Rosa et al., 2009). In particular, it is estimated that around 55 billion coconuts are produced annually worldwide. Most of their husks are abandoned, creating a waste of natural resources and a cause of environmental pollution (Gu, 2009). The coconut fibers (CFs), also referred as coir when completely ground up, are plant-derived NFs of the coconut fruit obtained from the palm tree (*Cocos nucifera* L.). The CFs are present in the mesocarp, which constitutes 30–35 wt.-% of the coconut (Tomczak, Sydenstricker, & Satyanarayana, 2007). Individual CFs show a length of 0.3–1.0 mm and a diameter of 0.01–0.02 mm, resulting in an average aspect ratio of approximately 35 (Hasan, Hoque, Mir, Saba, & Sapuan, 2015). The CFs are also characterized by a high toughness and durability as well as improved thermal stability due to their high lignin content (~40%) and relatively low cellulose content (~32%) (Rosa et al., 2010). These lignocellulosic fibers are not only abundant in tropical countries but also versatile, renewable, cheap, and biodegradable. Therefore, they could become potential substitutes for energy-intensive synthetic fibers in many applications where high strength and modulus are not required (Satyanarayana et al., 1982).

The CFs have been tested as reinforcing fillers upon the formulation of different thermoplastic materials, such as low-density polyethylene (LDPE) (Choudhury, Kumar, & Adhikari, 2007; Owolabi & Czvikovszky, 1988) and linear low-density polyethylene (LLDPE) (Choudhury et al., 2007), polypropylene (PP) (Gu, 2009; Hasan et al., 2015; Mir, Nafsin, Hasan, Hasan, & Hassan, 2013; Owolabi & Czvikovszky, 1988; Wambua, Ivens, & Verpoest, 2003), poly(vinyl chloride) (PVC) (Owolabi & Czvikovszky, 1988), starch–gluten (Corradini, Rosa, Mazzetto, Mattoso, & Agnelli, 2006), natural rubber (NR) (Geethamma, Thomas Mathew, Lakshminarayanan, & Thomas, 1998), among others. These previous studies have demonstrated that the incorporation of both untreated and chemically modified CFs into polymer formulations can represent a feasible route to produce low-cost composites with a moderate improvement of the mechanical properties. Interestingly, the CFs are exceptionally hydrophilic as they contain strongly polarized hydroxyl groups on their surface (Westerlind & Berg, 1988). CFs are thus inherently capable to adsorb and hold moisture up to 7–9 times their weight, being proposed as biosorbents for water treatment (Bhatnagar, Vilar, Botelho, & Boaventura, 2010). The outstanding capacity of the CFs to retain water and other polar components certainly opens up new attractive opportunities for potential uses as vehicle of functional and bioactive substances.

The particular chemical and morphological characteristics of the CFs can be explored to adsorb essential oils (EOs), *i.e.* aromatic and volatile oily liquids obtained from herbs and spices. Most EOs and their constituents are categorized as Generally Recognized as Safe (GRAS) by the U.S. Food and Drug Administration (López, Sánchez, Batlle, & Nerín, 2007). Among EOs, oregano essential oil (OEO), extracted from *Origanum vulgare* L., is well-recognized for its antioxidative and antimicrobial action in the food industry (Hosseini, Zandi, Rezaei, & Farahmandghavi, 2013). The biocide performance of OEO has been mainly attributed to its rich composition in phenolic compounds, namely carvacrol (up to 80%), thymol (up to 64%), and the monoterpene hydrocarbons γ-terpinene and p-cymene (both up to 52%) (Burt, 2004). The incorporation of OEO in plastic films to avoid microbial food spoilage currently represents an attractive option for packaging manufacturers. Several studies have demonstrated its efficacy in inhibiting microbial development and synthesis of microbial metabolites, including pathogenic bacteria, yeasts, and molds (Benavides et al., 2012; Hosseini, Rezaei, Zandi, & Farahmandghavi, 2015; Oussalah, Caillet, Salmiéri, Saucier, & Lacroix, 2004; Pelissari, Grossmann, Yamashita, & Pineda, 2009; Seydim & Sarikus, 2006; Zivanovic, Chi, & Draughon, 2005). Besides imparting antimicrobial characteristics to the films, OEO can change flavor, aroma, and odor. Nevertheless, similarly as with other EOs, OEO is volatile and easily evaporates and/or decomposes during processing and preparation of the antimicrobial films. Therefore, its direct exposure to heat, pressure, light or oxygen is a technological challenge.

The objective of the present study was to originally explore the inherent capacity of the CFs to adsorb and hold polar components in order to develop, by conventional melt-processing methodologies, PHBV-based green composite sheets with antimicrobial properties of interest in active packaging applications. To this end, the first part of the study was focused on optimizing the processing conditions of the green composites. In particular, it was analyzed the effect of varying both the CF weight content and the screw speed during melt processing on the aspect ratio and dispersion of the fibers in the PHBV matrices. In the second part, for the optimal processing conditions, the thermal, mechanical, and barrier properties of the compression-molded PHBV sheets were evaluated as a function of the CF content. In the last part, the CFs were impregnated with OEO by an innovative spray coating methodology, incorporated again into PHBV, and the antimicrobial properties of the green composite sheets were evaluated.

2. Experimental

2.1. Materials

Bacterial aliphatic copolyester PHBV was ENMAT™ Y1000 P, produced by Tianan Biologic Materials (Ningbo, China) and distributed by NaturePlast (Ifs, France). The product was delivered as off-white pellets packaged in plastics bags. The biopolymer resin presents a true density of 1.23 g/cm^3 and a bulk density of 0.74 g/cm^3, as determined by ISO 1183 and ISO 60, respectively. The melt flow index (MFI) is 5–10 g/10 min (190 °C, 2.16 kg), as determined by ISO 1133. The molar fraction of HV in the copolymer is 2–3%, whereas the weight-average molecular weight (M_W) is approximately 2.8×10^5 g/mol. According to the manufacturer, this resin is suitable for injection molding, thermoforming, and extrusion.

CFs were kindly supplied by Amorim Isolamentos, S.A. (Mozelos, Portugal) in the form of a liner roll. The fibrous layers were obtained from ripe coconuts, which were manually de-husked from the hard shell by driving the fruit down onto a spike to split it. 100% pure OEO was purchased from Gran Velada S.L. (Zaragoza, Spain) while food-grade paraffinic oil (grade 9578) was obtained from Quimidroga S.A.

Fig. 1. (a) As-received reel of coconut fibers (CFs); (b) Ground CFs; (c) Sieved CFs.

(Barcelona, Spain). 2,2,2-trifuoroethanol (TFE) with 99% purity, D-limonene with 98% purity, Nile Red (9-diethylamino-5H-benzo-α-phenoxazine-5-one), and dimethyl sulfoxide (DMSO) anhydrous with purity ≥99.9% were all purchased from Sigma-Aldrich S.A. (Madrid, Spain). All chemical reagents were utilized as received.

2.2. Fibers functionalization

CFs were initially separated from the roll and chopped to a length of *ca.* 5 mm in a Granulator 20-18/JM from Grindo S.R.L. (Cologno Monzese, Italy). Chopped fibers were then sieved using a Test sieve model from Controls S.p.A. (Milano, Italy) with an aperture of 2 mm. The resultant bulk density of the CFs was 0.14 g/cm^3, as determined by ISO 60. Fig. 1 shows the different stages followed for the preparation of the CFs.

Part of the obtained CFs was impregnated with OEO in order to provide them with antibacterial functionality, the here so-called functionalization. For this purpose, a 2:1 (vol./vol.) paraffinic oil/OEO solution was prepared, as this was the highest OEO content without creating phase separation. This solution, with a density of 0.902 g/mL, was added at 15 wt.-% to the CFs by means of an air spray gun from Nutool (Doncaster, UK) connected to a 24 l 1.0HP PWB24S air compressor from PowerED® (Amiais de Baixo, Portugal) working at 2 bar. This way, the dried CFs were sprayed every 5 s while rotating at 58 rpm inside a drum attached to an ARTISAN 5KSM125EER household mixer from KitchenAid® (Michigan, USA).

2.3. Preparation of green composites

Prior to melt processing, the PHBV pellets and CFs were dried for 4 h at 80 °C in an oven to remove the residual humidity. Then, different PHBV formulations were melt compounded by twin-screw extrusion (TSE) varying the CF content, *i.e.* 0, 1, 3, 5, and 10 wt.-%, in a co-rotating intermeshing twin-screw extruder LSM 34 G l from Leistritz AG (Nuremberg, Germany). The screws have a diameter (D) of 34 mm and a length-to-diameter ratio (L/D) of 29. The modular barrel is equipped with 8 individual heating zones and is coupled to a strand die. The extruder layout with the detailed screw configuration is presented in Fig. 2. Basically, the screw contains two mixing zones, each consisting of a series of kneading disks staggered at 90° (in order to induce dispersion), that are separated by conveying sections that work mostly partially filled. The components are fed separately upstream of each mixing zone. The PHBV pellets were fed into the main hopper with a volumetric DVM18-L feeder from Moretto S.p.A. (Massanzago, Italy) at a feeding rate of 2 kg/h. The CFs were first pre-mixed in a zipped bag with 1 part per hundred resin (phr) of paraffinic oil and then introduced in the extruder after melting the polymer, at L/D = 12, through the side feeder. As commonly faced with other low-density fibers, there were difficulties in guaranteeing a precise and constant feeding throughput. A venting port at L/D = 23 coupled to a vacuum pump enabled the removal of both residual moisture and volatiles. Three different screw speeds were tested, *i.e.* 75, 150, and 225 rpm, and the following decreasing temperature profile was fixed (from hopper to die): 195/190/185/180/175/170/165/160 °C. The extruded strand was cooled in a water bath, dried with an air-knife, and then pelletized by a rotary cutter. The minimum residence time was estimated by measuring the time that a blue masterbatch pellet would take from being introduced directly into the extruder until exiting from the die.

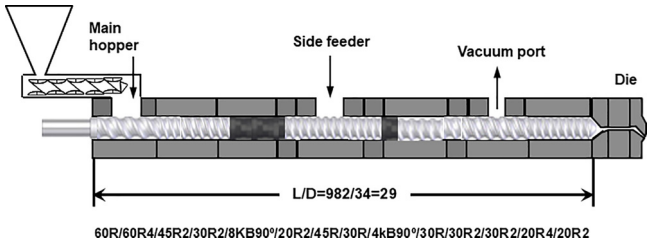

Fig. 2. Detailed cylinder with screw configuration.

The compounded pellets were shaped into sheets with a thickness of ~500 μm by compression molding using a hydraulic press from Geo E. Moore & Son (Bham.) Ltd. (Birmingham, UK). About 10 g of material were placed in a hollow aluminum mold of 10 × 10 cm^2 and then introduced into the press. Materials were initially preheated at 190 °C for 1 min, without pressure, and subsequently hot-pressed for 3 min at 4 tons. Finally, the samples were cooled down to 25 °C by means of an internal water circulating system.

2.4. Characterization methods

2.4.1. Sheet thickness and samples conditioning

The thickness of the compression-molded sheets was measured with a digital micrometer series S00014 from Mitutoyo Corporation (Kawasaki, Japan), having ± 0.001 mm accuracy, at five random positions. Samples were aged for at least 15 days prior to any physical characterization in a desiccator at 25 °C and 0% relative humidity (RH).

2.4.2. Optical microscopy

Dispersion quality of CFs in the green composites was assessed with a light transmission optical microscope Olympus BH-2 from Olympus Optical Co., Ltd (Tokyo, Japan), coupled to a digital camera system Leica DFC280 from Meyer Instruments, Inc. (Houston, Texas, USA). Fiber attrition was investigated by monitoring fiber length distribution on the PHBV composites processed with different CF contents and at different conditions. This method was performed by immersing a small sample of each specimen in TFE solvent at room temperature for 12 h. The resultant solution was centrifuged and filtered so that PHBV was removed and the recovered CFs were deposited onto microscopy glass slabs for observation.

The OEO-containing CFs were analyzed by fluorescence microscopy using an Olympus BX51 from Olympus Optical Co., Ltd. The samples were previously dyed with Nile Red, a lipophilic dye, in a 0.25 mg/ml solution of DMSO at 1:10 dye/sample (vol./vol.), covered in aluminum foil to protect them from light exposure, and dried at 25 °C for at least 12 h prior to observation. The samples were analyzed at an emission wavelength between 470 and 490 nm.

2.4.3. Melt flow index

MFI of the neat PHBV and its green composites pellets were measured at 185 °C with a load of 1.2 kg using a MFI Daventest LPF-002 from Lloyd Instruments Ltd. (Bognor Regis, UK). Higher temperatures and weights triggered excessive mass outputs that impaired measurement accuracy. Data were reported as the mean value and standard error computed from 10 tests.

2.4.4. Thermal analysis

Thermal transitions were analyzed by differential scanning calorimetry (DSC) on a DSC-7 analyzer from PerkinElmer, Inc. (Waltham, MA, USA), equipped with a cooling accessory Intracooler 2 also from PerkinElmer, Inc. A heating step from −30 to 200 °C was followed by a cooling step to −30 °C under nitrogen atmosphere with a flow-rate of 20 mL/min. The scanning rate was 10 °C/min and an empty aluminum pan was used as reference. Calibration was performed using an indium sample. All tests were carried out at least in triplicate. The glass transition temperature (T_g), cold crystallization temperature (T_{cc}), enthalpy of cold crystallization (ΔH_{cc}), melting temperature (T_m), and enthalpy of melting (ΔH_m) were obtained from the first heating scan, while the crystallization temperature from the melt (T_c) and enthalpy of crystallization (ΔH_c) were determined from the cooling scan. The percentage of crystallinity (X_c) was determined using the following expression:

$$Xc = \left[\frac{\Delta Hm - \Delta Hcc}{\Delta H_m^0 \bullet (1\text{-}w)} \right] \bullet 100 \quad (1)$$

where ΔH_m° = 146.6 J/g is the enthalpy corresponding to the melting of a 100% crystalline PHB sample (Barham, Keller, Otun, & Holmes, 1984) while the term 1-*w* represents the biopolymer weight fraction in the composite.

Thermogravimetric analysis (TGA) was performed in a TG-STDA model TGA/STDA851e/LF/1600 thermobalance from Mettler-Toledo, LLC (Columbus, OH, USA). The samples, with a weight of ~15 mg, were heated from 50 to 900 °C at a heating rate of 10 °C/min under a nitrogen flow-rate of 50 mL/min.

2.4.5. Tensile tests

Dumbbell 500 μm-thick samples were die-cut from the compression-molded sheets and conditioned to ambient conditions, *i.e.* 25 °C and 50% RH, for 24 h. Tensile tests were carried out at room temperature in a universal mechanical testing machine AGS-X 500 N from Shimadzu Corp. (Kyoto, Japan) in accordance with ASTM D638 (Type IV) standard. This was equipped with a 1-kN load cell and the cross-head speed was 10 mm/min. A minimum of six specimens were measured for each sample.

2.4.6. Permeability tests

The water vapor permeability (WVP) and limonene permeability (LP) were determined according to the ASTM 2011 gravimetric method. In the case of WVP, 5 ml of distilled water were poured into a Payne permeability cup (∅ = 3.5 cm) from Elcometer Sprl (Hermalle-sous-Argenteau, Belgium). The sheets were placed in the cups so that on one side they were exposed to 100% RH, avoiding direct contact with water. The cups containing the sheets were then secured with silicon rings and stored in a desiccator at 25 °C and 0% RH. Identical cups with aluminum foils were used as control samples to estimate water loss through the sealing. The cups were weighed periodically using an analytical balance with ± 0.0001 g accuracy. Water vapor permeation rate (WVPR), also called water permeance when corrected for permeant partial pressure, was determined from the steady-state permeation slope obtained from the regression analysis of weight loss data per unit area *versus* time, in which the weight loss was calculated as the total cell loss minus the loss through the sealing. WVP was obtained, in triplicate, by correcting the permeance by the average sheet thicknesses.

For LP, similarly, 5 ml of D-limonene was placed inside the Payne permeability cups and the cups containing the sheets were stored under controlled conditions, *i.e.* 25 °C and 40% RH. Limonene permeation rate (LPR) was obtained from the steady-state permeation slopes and the weight loss was calculated as the total cell loss minus the loss through the sealing plus the water sorption gained from the environment measured in samples with no permeant. LP was calculated taking into account the average sheet thickness in each case, measuring three replicates per sample.

Oxygen permeability (OP) was obtained from the oxygen transmission rate (OTR) measurements, recorded in duplicate, using an Oxygen Permeation Analyzer M8001 from Systech Illinois (Thame, UK) at 25 °C and 60% RH. The samples were previously purged with nitrogen in the humidity equilibrated samples and then exposed to an oxygen flow of 10 mL/min. The exposure area during the test was 5 cm^2. Sheet thickness and gas partial pressure were determined. Measurements were performed in duplicate.

2.4.7. Antibacterial assays

The antibacterial activity of the neat OEO, the OEO-containing CFs, and the green composite sheets with the OEO-containing CFs was evaluated against *Staphylococcus aureus* (*S. aureus*) ATCC 6538 P. This bacterial strain was obtained from the Spanish Type Culture Collection (CECT) (Valencia, Spain) and it was cultivated at optimal growth conditions in tryptone soy broth (TSB) from Oxoid Thermo Scientific (Basingstoke, UK), having a concentration of 6.3 × 10^8 colony forming units (CFU)/ml. Previous to each study, a 100-μl aliquot from the culture was transferred to TSB and grown at 37 °C to the mid-exponential phase of growth with an approximate count of 5 × 10^5 CFU/ml. To ensure sterilization, all materials were initially exposed to ultraviolet (UV) radiation for 30 min in a Biostar cabinet from Telstar S.A. (Madrid, Spain).

The effectiveness of the OEO and OEO-containing CFs against *S. aureus* was tested following the plate micro-dilution protocol, as described in the Methods for Dilution Antimicrobial. Susceptibility Tests for Bacteria That Grow Aerobically; Approved Standard—Tenth. Edition (M07-A10) by the Clinical and Laboratory Standards Institute (CLSI). For this, a 96-well plate with an alpha numeric coordination system (columns 1–12 and rows A-H) were used, where 10 μl of the tested samples were introduced in the wells with 90 μl of the bacteria medium. In the wells corresponding to A, B, C, E, F, and G columns different concentrations of OEO, *i.e.* 0.078, 0.156, 0.312, 0.625, 1.25, 2.5, 5, 10, 20, and 40 μl/ml, and of OEO-containing CFs, *i.e.* 0.315, 0.625, 1.25, 2.5, 5, 10, 25, 50, 100, and 250 μg/ml were tested, in triplicate, from rows 1 to 10. Columns D and H were used as the control of OEO and OEO-containing CFs, respectively, without bacteria. Row 11 was taken as the positive control, *i.e.* only TSB, and row 12 was used as the negative control, *i.e. S. aureus* in TSB. The plates were incubated at 37 °C for 24 h. Thereafter, 10 μl of resazurin solution, 100 μg/ml in TBS, a metabolic indicator obtained from MP Biomedicals, LLC (Illkirch, France), was added to each well and incubated again at 37 °C for 2 h. Upon obtaining the resazurin change, the wells were read through color difference. The minimum inhibitory concentration (MIC) was determined as the lowest concentration of OEO and OEO-containing CFs presenting growth inhibition.

A modification of the Japanese Industrial Standard (JIS) Z 2801:2010 was performed to evaluate the bacterial efficiency on the sheets surface. This technique is useful to determine the antimicrobial activity of finished products, particularly including polymer composite pieces (Torres-Giner, Torres, Ferrándiz, Fombuena, & Balart, 2017). Briefly, a bacterial suspension of *S. aureus* of about 5 × 10^5 CFU/mL was spread uniformly on the surface of sheets with dimensions of 2 × 2 cm^2 and then covered by an inert 10-μm LDPE film of 1.5 × 1.5 cm^2. After 24 h of incubation at 95% RH, bacteria were recovered with phosphate-buffered saline (PBS), inoculated onto tryptic soy agar (TSA) plates, and incubated at 37 °C for 24 h to quantify the number of viable bacteria. PHBV sheets with different CF contents were

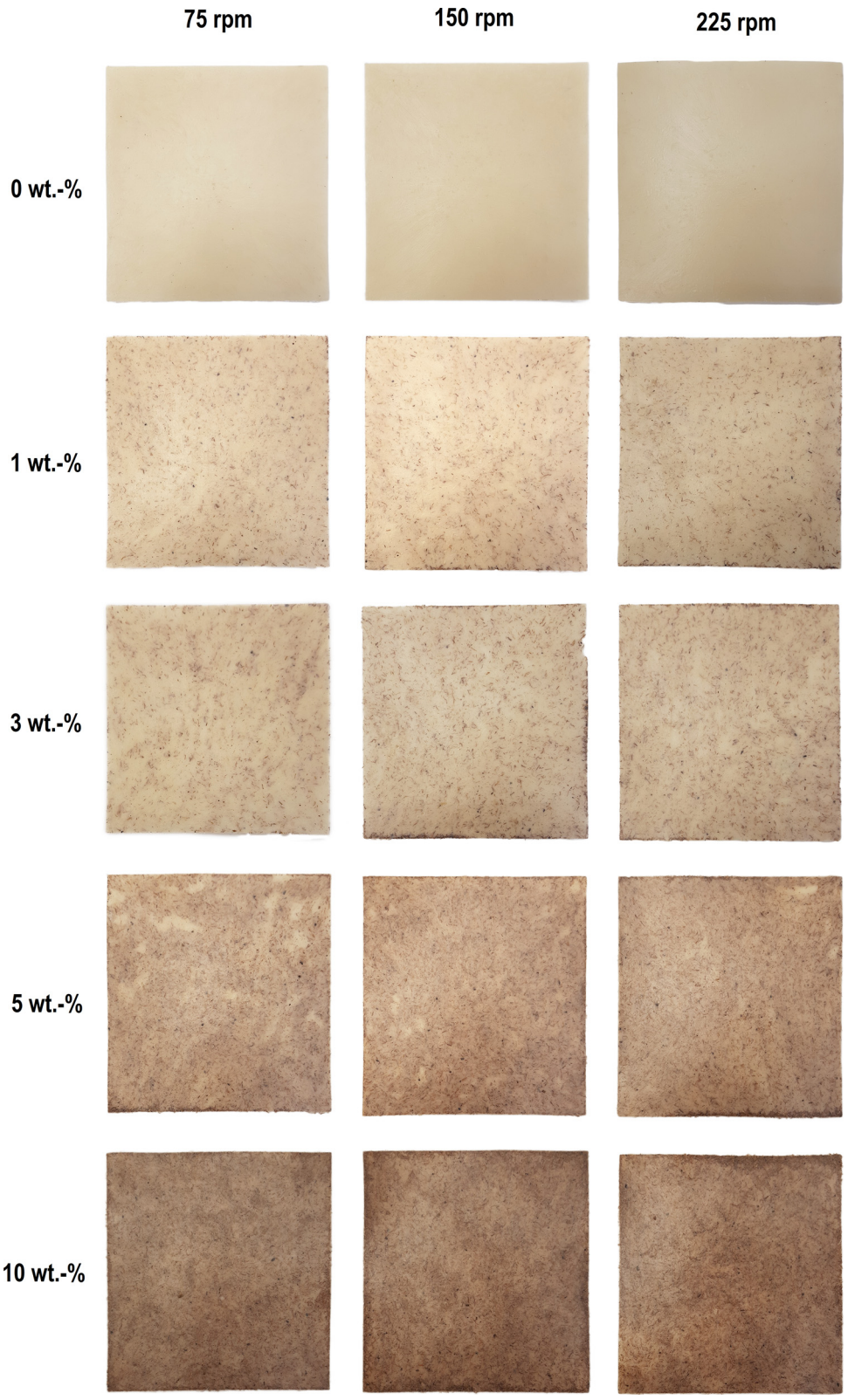

Fig. 3. Surface appearance of the compression-molded sheets as a function of the poly(3-hydroxybutyrate-*co*-3-hydroxyvalerate) (PHBV) and coconut fibers (CFs) weight content and screw speed.

analyzed, using both sheets without fibers and with fibers without OEO as the negative controls. The antimicrobial activity was evaluated as synthesized, *i.e.* 1 day after preparation, and 15 days later. Surface reduction (R) was calculated as follows:

$$R = \left[\log\left(\frac{B}{A}\right) - \log\left(\frac{C}{A}\right)\right] = \log\left(\frac{B}{C}\right) \quad (2)$$

where A is the average of the number of viable bacteria on the control sample immediately after inoculation, B is the average of the number of

viable bacteria on the control sample after 24 h, and C is the average of the number of viable bacteria on the test sample after 24 h. Three replicate experiments were performed for each sample and the antibacterial activity was evaluated with the following assessment: Non-significant ($R < 0.5$), slight ($R \geq 0.5$ and < 1), significant ($R \geq 1$ and < 3), and strong ($R \geq 3$).

3. Results and discussion

3.1. Melt processability

Fig. 3 shows the surface view of the green composite sheets varying the CF contents and processed at different processing conditions. In all cases, the green composite sheets exhibited a smooth, defect-free, and uniform surface, in which CFs appeared randomly dispersed. Distribution was relatively uniform, albeit some small areas seem to contain lower CF concentration. As expected, the CF content highly influenced on the color intensity of the PHBV sheets. Then, sheets produced with the highest CF contents, *i.e.* 5 and 10 wt.-%, presented a wood-like visual feature, which could be aesthetically suitable to imitate solid wood parts for boards, lids or containers of interest in, for instance, rigid packaging. In contrast, the processing conditions had a minor influence on both surface aspect and distribution of the CFs into the PHBV matrix. Only the sheets obtained from green composites compounded at 225 rpm presented a slight color increase, which was probably caused by thermal degradation arising from the viscous dissipation associated to flow under higher shear-rates.

CFs in the green composite sheets were imaged by optical microscopy, after dissolving and filtrating PHBV. Representative pictures are displayed in Fig. 4. Residence time and fiber dimensions were evaluated in order to select the optimal screw speed for which the set temperature and feed-rate were kept constant. Table 1 reports both characteristics for each composition and screw speed. As expected, at a given feed-rate, residence time was gradually reduced with increasing screw speed, as flow along the screw was more effective and the number of fully filled channels decreased. For instance, for the neat PHBV formulation, residence time decreased from 131 s, at 75 rpm, to 97 s and 64 s, at 150 rpm and 225 rpm, respectively. The incorporation of CFs slightly increased the residence time due to their lower bulk density in relation to the PHBV pellets, *i.e.* the total volume occupied by the material in the extruder increased though the output remained constant. For all processing conditions, CFs presented a similar diameter, varying in the range 100–400 μm and with a mean value of approximately 215 μm, whereas their length significantly decreased with increasing both the content and screw speed. Specifically, the average fiber length decreased from above 1900 μm, for the composite formulations with 1 wt.-% CFs, down to below 600 μm, for those containing 10 wt.-% CFs. This corresponds to a decrease of the fiber aspect ratio from approximately 9 to 2.5. Fiber lengths also decreased with increasing the screw speed, which is expected as stresses are larger for faster screw speeds. Interestingly, the green composite with 10 wt.-% CFs presented the highest fiber length at 150 rpm, *i.e.* approximately 1179 μm, and also the lowest at 75 rpm, *i.e.* approximately 542 μm.

In order to correlate fiber attrition to melt viscosity, MFI was evaluated on the PHBV samples processed at 150 rpm. As one can observe in Fig. 5, the MFI values decreased with increasing the CFs content. This means that melt viscosity of the composite formulations was higher than the neat PHBV formulation and, thus, the intensity of the thermomechanical stresses raised. This was mainly related to the intensification of fiber-to-fiber collisions. While fiber dispersion requires stresses to be larger than the cohesive strength of the aggregates, larger stresses can also favor fibers rupture (Torres-Giner, 2016). As a result, composites formulated with more CFs presented higher viscosity and lower lengths. However, the lowest MFI value was observed for the composite formulation with 3 wt.-% CFs and then it increased for the larger CF contents. This viscosity decrease at high CF contents suggests an increase of biopolymer degradation or melt-shear thinning due to the presence of more fibers, which is known to occur in PHBV materials (Hilliou et al., 2016). Therefore, the complex interplay concerning reduced melt viscosity at higher CF contents, high residence times at low screw speeds, and thermal degradation of PHBV due to possible viscous heating, may explain the non-trivial evolution of fiber length.

From the above and within the experimental window tested herein, it was observed that the optimal screw speed to process the PHBV/CFs composites is 150 rpm. This processing condition delivered the most balanced fiber distribution, average fiber length, and intermediate residence times. In particular, the fiber aspect ratio remained in the 5.5–9.0 range, decreasing with increasing the CF content, and the residence time was of the order of 100 s. It can be thus considered that this processing condition could be beneficial to process both thermally sensitive PHBV and thermolabile additives.

3.2. Sheets characterization

The green composite formulations melt-compounded at 150 rpm were thereafter compression-molded into sheets and these were characterized in terms of their thermal, mechanical, and barrier properties.

Table 2 summarizes the thermal properties determined by DSC and TGA. Within the experimental precision, all PHBV sheets presented similar values of T_g, T_c, and T_m (about −3 °C, 121 °C, and 173 °C, respectively). Similar results have been reported in the literature for other PHBV materials, indicating that the HV content plays the major role in defining the thermal transitions (Shang et al., 2012). In addition, cold crystallization was not observed and all the samples crystallized from the melt in a single peak. Interestingly, the presence of the CFs significantly affected the biopolymer degree of crystallization. While the neat PHBV sheet presented a X_c of approximately 54%, the addition of 1–5 wt.-% CFs reduced it to values in the 45–50% range and X_c increased to about 58% for the 10 wt.-% CF content. This result suggests that crystal growth in the green composites was controlled by two competing factors, namely nucleation and confinement. As with other PHBV composites (Cunha et al., 2015), the presence of low contents of long fibers inhibited the chain-folding process of PHBV molecules, hindering molecular organization at the crystal growth front. Conversely, the existence of a high content of shorter fibers seems to provide a nucleating effect. The latter can be related to the degradation process triggered by the high CF content, as explained above, by which PHBV molecules were shorter and, thus, easier to crystallize.

Concerning the TGA data, also listed in Table 2, one can observe that thermal decomposition of the PHBV composites started in the range of 270–280 °C, presenting a degradation temperature (T_{deg}) close to 300 °C with a mass loss of approximately 70%. The incorporation of CFs slightly reduced the thermal stability of PHBV, but it also delayed the amount of mass loss during degradation. It is also worthy to note that the amount of residual mass increased, approximately from 3% to 6%, which can be related to the presence of inorganic impurities in the fibers. In general, the addition of CFs up to 10 wt.-% did not significantly alter the thermal degradation profile of PHBV, thus, positively not impairing its processing window.

Table 3 shows the tensile properties of PHBV and its green composite with CFs. The neat PHBV sheet presented a tensile modulus of *ca.* 3.7 GPa, a tensile strength of *ca.* 34 MPa, and an elongation at break of *ca.* 1.2%. These properties clearly indicate that the PHBV sheets were rigid and brittle. As expected, the incorporation of CFs further increased, though not significantly, the tensile modulus and also reduced both the tensile strength and elongation at break. The same response has been reported for other compression-molded green composite sheets based on PHAs (Shibata, Oyamada, Kobayashi, & Yaginuma, 2004; Torres-Giner, Montanes, Fombuena, et al., 2016), which have been mainly related to a poor fiber–matrix adhesion. The 5 wt.-% CF-containing sheet presented the highest tensile modulus, *i.e.* approximately 4.1 GPa, with tensile strength and elongation-at-break values of

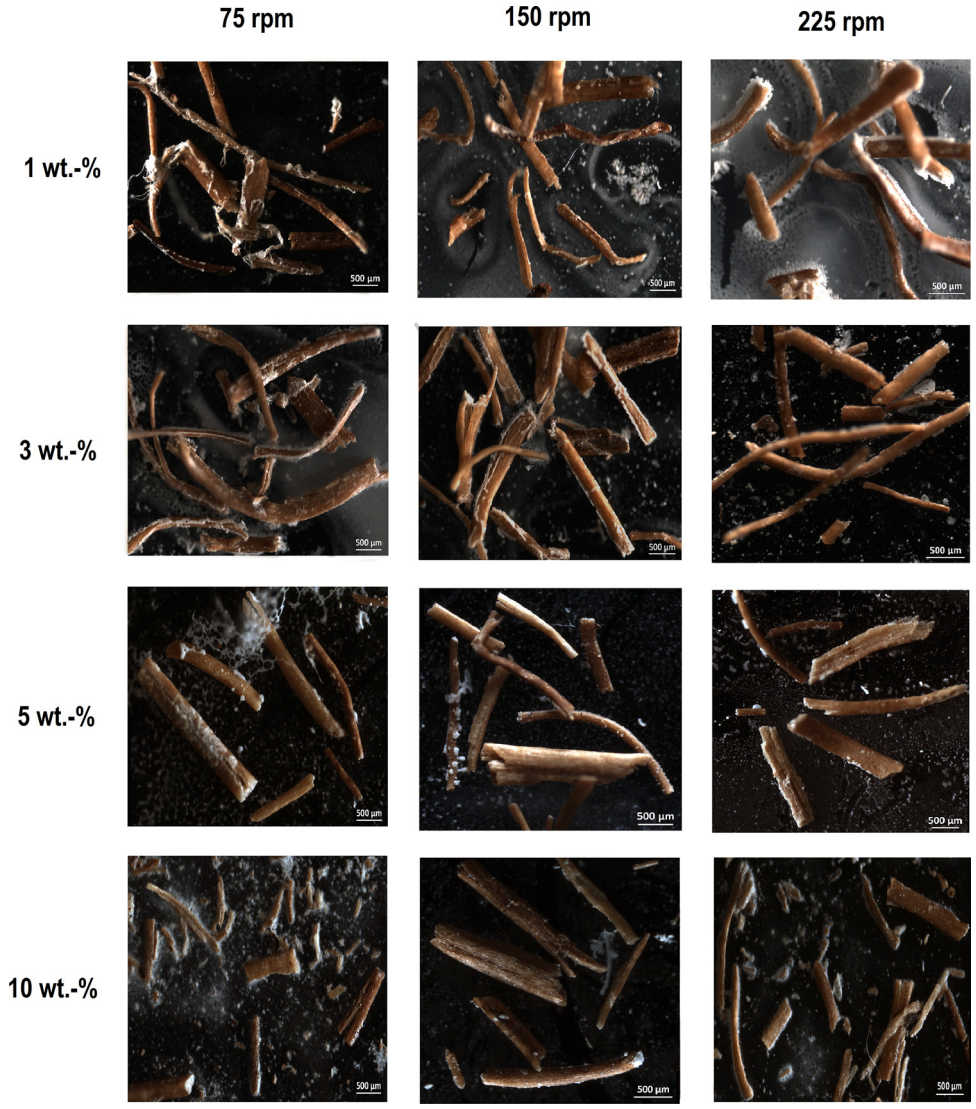

Fig. 4. Optical microscopy images of the coconut fibers (CFs) extracted from the green composite sheets at different weight contents and screw speed. Scale markers of 500 µm.

Table 1
Residence time (t_R) and mean fiber length during melt compounding as a function of the poly(3-hydroxybutyrate-*co*-3-hydroxyvalerate) (PHBV) and coconut fibers (CFs) content and screw speed.

PHBV content (wt.-%)	CF content (wt.-%)	Screw speed (rpm)	t_R (s)	Fiber length (µm)
100	0	75	131 ± 3	–
100	0	150	97 ± 2	–
100	0	225	64 ± 1	–
99	1	75	132 ± 5	1914.5 ± 686.3
99	1	150	98 ± 3	1848.4 ± 634.6
99	1	225	65 ± 1	1486.2 ± 451.3
97	3	75	134 ± 4	1784.3 ± 718.9
97	3	150	100 ± 1	1711.6 ± 505.4
97	3	225	66 ± 2	1404.5 ± 683.4
95	5	75	136 ± 5	1760.4 ± 446.5
95	5	150	102 ± 2	1633.4 ± 491.6
95	5	225	68 ± 1	1309.6 ± 671.7
90	10	75	143 ± 5	542.3 ± 190.8
90	10	150	106 ± 3	1178.9 ± 333.9
90	10	225	70 ± 2	715.2 ± 302.2

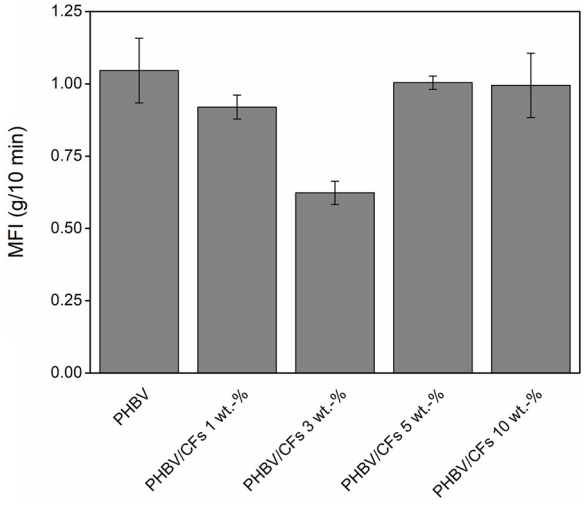

Fig. 5. Melt flow index (MFI) of the green composite pellets as function of the weight content of coconut fibers (CFs). Test performed at 185 °C with a load of 1.2 kg.

Table 2
Thermal properties of the compression-molded sheets made of poly(3-hydroxybutyrate-*co*-3-hydroxyvalerate) (PHBV) and coconut fibers (CFs). The glass transition temperature (T_g), melting temperature (T_m), and normalized enthalpy of melting (ΔH_m) were obtained from the differential scanning calorimetry (DSC) curves during the first heating scan while the crystallization temperature (T_c) and normalized crystallization (ΔH_c) from the cooling scan. The onset degradation temperature, defined as the temperature at 5% weight loss ($T_{5\%}$), degradation temperature (T_{deg}), and residual mass at 900 °C were obtained from the thermogravimetric analysis (TGA) curves.

Samples	DSC parameters						TGA parameters			
	T_g (ºC)	T_c (ºC)	T_m (ºC)	ΔH_c (J/g)	ΔH_m (J/g)	X_c (%)	$T_{5\%}$ (ºC)	T_{deg} (ºC)	Mass loss (%)	Residual mass (%)
PHBV	−3.3 ± 0.8	120.6 ± 0.1	172.8 ± 0.2	84.7 ± 2.4	79.4 ± 0.9	54.1 ± 0.6	277 ± 0.3	298 ± 0.5	72.19 ± 0.6	3.2 ± 0.2
PHBV/CFs 1 wt.-%	−2.4 ± 0.3	120.2 ± 0.9	173.8 ± 1.3	78.3 ± 4.2	64.9 ± 1.1	44.7 ± 0.8	276 ± 0.5	296 ± 0.5	70.99 ± 0.3	3.5 ± 0.2
PHBV/CFs 3 wt.-%	−2.3 ± 0.9	120.4 ± 1.1	173.9 ± 1.4	74.3 ± 4.4	66.6 ± 3.5	46.9 ± 0.5	275 ± 0.4	295 ± 0.4	70.78 ± 0.4	3.5 ± 0.3
PHBV/CFs 5 wt.-%	−2.2 ± 0.4	121.0 ± 0.6	172.9 ± 0.5	75.5 ± 2.6	69.8 ± 2.7	50.1 ± 0.9	274 ± 0.5	293 ± 0.3	64.85 ± 0.5	4.6 ± 0.3
PHBV/CFs 10 wt.-%	−1.8 ± 0.6	119.8 ± 0.5	172.5 ± 1.0	76.8 ± 3.0	76.8 ± 3.2	58.2 ± 1.4	273 ± 0.4	291 ± 0.4	63.79 ± 0.3	5.8 ± 0.2

Table 3
Mechanical properties of the compression-molded sheets made of poly(3-hydroxybutyrate-*co*-3-hydroxyvalerate) (PHBV) and coconut fibers (CFs) in terms of tensile modulus (E), tensile strength at yield (σ_y), and elongation at break (ε_b).

Sample	E (MPa)	σ_y (MPa)	ε_b (%)
PHBV	3671 ± 180	33.8 ± 2.1	1.18 ± 0.15
PHBV/CFs 1 wt.-%	3815 ± 164	30.7 ± 3.4	1.06 ± 0.10
PHBV/CFs 3 wt.-%	3916 ± 288	29.3 ± 2.0	0.95 ± 0.04
PHBV/CFs 5 wt.-%	4093 ± 197	28.6 ± 2.0	0.88 ± 0.12
PHBV/CFs 10 wt.-%	3720 ± 125	24.7 ± 1.3	0.67 ± 0.09

approximately 29 MPa and 0.9%, respectively. It is also worthy to mention the low elastic modulus observed for the green composite sheet containing 10 wt.-% CFs, *i.e.* ~3.7 GPa, which can be related to the presence of fibers with lower mean fiber lengths, as previously shown in Table 1. The lowest values of tensile strength and elongation at break were also observed for the green composite sheet with 10 wt.-% CFs, *i.e.* approximately 25 MPa and 0.7%, respectively. Therefore, the CFs acted as an effective reinforcement of PHBV matrices when their length exceeds a critical threshold, in this case approximately 1500 µm, which corresponds to an aspect ratio close to 7. However, the exact mechanism for the reinforcement might go beyond the effect of fiber size, as both PHBV matrix thermal degradation and composite enhanced crystallinity in the sheet with 10 wt.-% CFs may add complexity to the mechanical–structural relationships.

Finally, the barrier properties to water vapor, limonene, and oxygen were determined and the permeability values are included in Table 4. The barrier performance is, in fact, one of the main parameters of application interest for food packaging. One can observe that the permeability to both water and limonene vapors slightly raised by increasing the CF content. Such increase was higher in the case of water vapor, reaching permeability values close to 4×10^{-15} kg m m^{-2} Pa^{-1} s^{-1}. Since water vapor is mainly a diffusivity-driven property in PHAs due to their low water sorption nature (Razumovskii, Iordanskii, Zaikov, Zagreba, & McNeill, 1994), the increase in permeability to water vapor can be ascribed to the hydrophilic character of the filler and possibly also to increased free volume at the fiber–matrix interface. To put these values into a more packaging context, WVP values of the here-developed green composite sheets are in the same order of magnitude as their petroleum-based counterpart polyethylene terephthalate (PET) films, *i.e.* 2.30×10^{-15} kg m m^{-2} Pa^{-1} s^{-1} (Lagaron, 2011).

Limonene transport properties are also important in packaging applications because this vapor is usually used as a standard system to test aroma barrier. The effect of fiber content on LP was relatively small and the neat PHBV and green composite sheets with CFs showed values in the range of 1.1–1.5 × 10^{-14} kg m m^{-2} Pa^{-1} s^{-1}. In this sense, limonene, as opposed to moisture, is a strong plasticizing component for PHAs and, then, solubility plays a more important role in permeability than diffusion. For example, Sanchez-Garcia, Gimenez, and Lagaron (2008) reported a limonene uptake of *ca.* 12.7 wt.-% for films made of PHBV with 12 mol.-% HV prepared by solvent casting, resulting in a LP value of 1.99×10^{-13} kg m m^{-2} Pa^{-1} s^{-1}. Interestingly, the here-prepared green composite sheets were 13–17 times more barrier to limonene, which can be ascribed to both the lower HV content of the here-used copolyester and also to the compression molding methodology. The observed increase in permeability when introducing CFs, though slight, may be related to a sorption phenomenon at the filler–matrix interface. In any case, the here-obtained PHBV-based sheets still presented LP values close to those previously reported for PHB films, *i.e.* 8.8×10^{-15} kg m m^{-2} Pa^{-1} s^{-1}, and approximately 8–10 times lower than PET films, *i.e.* 1.17×10^{-13} kg·m·m^{-2}·Pa^{-1}·s^{-1}, both obtained by compression molding (Sanchez-Garcia, Gimenez, & Lagaron, 2007).

In relation to oxygen, the presence of CFs induced a slight reduction in permeability though the trend was not monotonic. Since oxygen is a noncondensable small permeant, the presence of the cellulosic fibers can block oxygen diffusion while the heterogeneities within the composite can serve as preferential paths for the oxygen molecules. The highest barrier effect was observed for the PHBV/CFs 5 wt.-%, with a OP value of 1.73×10^{-19} m^3 m m^{-2} Pa^{-1} s^{-1}, which is close to that of PET films, *i.e.* 1.35×10^{-19} m^3 m m^{-2} Pa^{-1} s^{-1} (Lagaron, 2011). This suggests that, at this intermediate fiber content, the contribution of the blocking effect over the heterogeneities was optimal. Overall, the here-obtained PHBV-based composite sheets presented OP values in the 0.7–0.8 × 10^{-18} m^3 m m^{-2} Pa^{-1} s^{-1} range, being slightly lower than those recently observed for electrospun homopolyester PHB films (Cherpinski, Torres-Giner, Cabedo, Méndez, & Lagaron, 2017) but

Table 4
Barrier properties of the compression-molded sheets made of poly(3-hydroxybutyrate-*co*-3-hydroxyvalerate) (PHBV) and coconut fibers (CFs) in terms of water vapor permeability (WVP), limonene permeability (LP), and oxygen permeability (OP).

Sample	WVP x 10^{15} (kg m m^{-2} Pa^{-1} s^{-1})	LP x 10^{14} (kg m m^{-2} Pa^{-1} s^{-1})	OP x 10^{18} (m^3 m m^{-2} Pa^{-1} s^{-1})
PHBV	1.83 ± 0.47	1.17 ± 0.19	0.80 ± 0.14
PHBV/CFs 1 wt.-%	1.93 ± 0.34	1.19 ± 0.31	0.77 ± 0.09
PHBV/CFs 3 wt.-%	3.60 ± 0.46	1.25 ± 0.22	0.73 ± 0.08
PHBV/CFs 5 wt.-%	3.93 ± 0.58	1.38 ± 0.27	0.17 ± 0.06
PHBV/CFs 10 wt.-%	3.96 ± 0.57	1.48 ± 0.24	0.74 ± 0.05

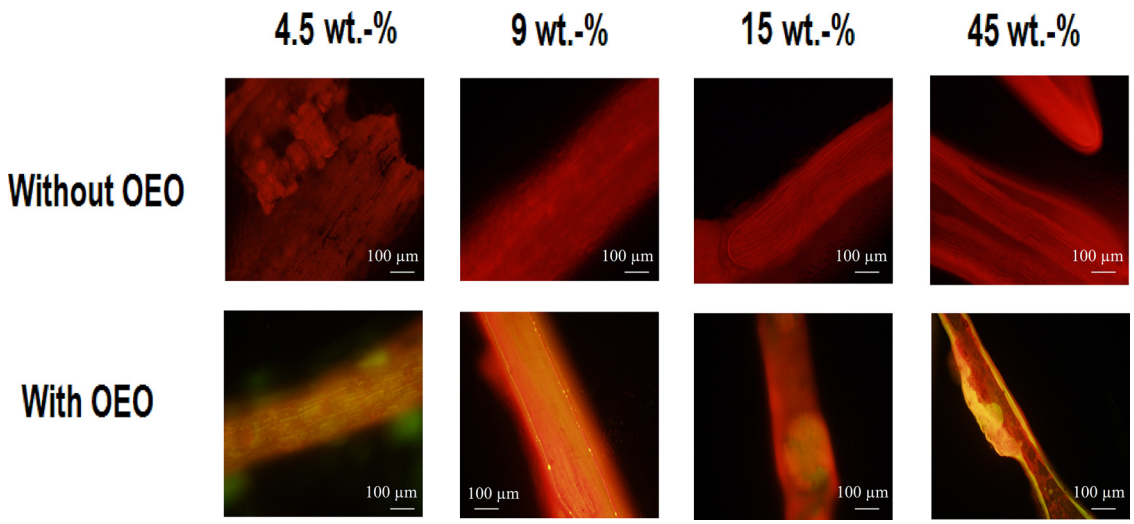

Fig. 6. Fluorescence microscopy images of the coconut fibers (CFs) impregnated with different weight contents of oil–oregano essential oil (OEO) mixture. Images were taken with an emission wavelength between 470 and 490 nm. Scale markers of 100 µm.

higher than conventional 100-µm PHB films prepared by compression molding (Sanchez-Garcia et al., 2007).

3.3. Antibacterial activity

In the last part of this study, the CFs were impregnated with different contents of an oil–OEO mixture by means of an in-house developed spraying methodology. Fig. 6 shows the fluorescence images taken by optical microscopy on the resultant OEO-containing fibers. One can observe that the oil–OEO mixture, shown as yellow-to-orange areas in the images, was homogenously distributed along the fibers surface for contents up to 15 wt.-%. However, at the highest tested content, *i.e.* 45 wt.-%, the oily extract eventually saturated the fibers and accumulated around their outer surface. Based on this observation, the CFs containing 15 wt.-% oil–OEO mixture, which in turns provided a final content of 5 wt.-% OEO, were selected to further functionalize the green composites with antibacterial properties. As the CF content in the biopolymer was kept at 1–10 wt.-%, this resulted in a concentration range of 0.05–0.5 wt.-% OEO in the PHBV sheets.

The MIC values, defined as the lowest concentration of a biocide substance that is capable of inhibiting bacterial growth, of both the neat OEO and OEO-containing CFs were determined using the plate microdilution protocol. While the neat OEO presented a MIC value against *S. aureus* of 0.312 µl/ml, this value was significantly higher for the OEO-containing CFs, *i.e.* 25 µg/ml, which corresponds to a OEO concentration of 1.25 µg/ml. This reduction in antibacterial effectiveness, of about 4 times, can be related to partial losses during the spraying process, a heterogeneous distribution of the OEO, and/or to an in-depth entrapment of the antibacterial oil into fibers regions that were not accessible for interaction with bacteria (*e.g.* pores). It is also worthy to indicate that the here-reported MIC values for OEO were relatively low, being for instance one order of magnitude lower than those reported by dos Santos Rodrigues et al. (2017) against different planktonic and sessile cells of *S. aureus* isolates.

In relation to the possible biological mechanism exerted by OEO on *S. aureus*, Dadalioğlu and Evrendilek (2004) attributed this effect to two particular components: the phenolic compound carvacrol and the monoterpene p-cymene. According to Zivanovic et al. (2005), the proposed action of phenolic compounds is based on their attack on the phospholipid cell membrane, which causes increased permeability and leakage of cytoplasm, or on their interaction with enzymes located at the cell wall. Indeed, most studies investigating the antibacterial activity of OEO agree that, generally, the extract is slightly more active against Gram-positive (G+) than Gram-negative (G−) bacteria (Burt, 2004; Hosseini et al., 2015; Zivanovic et al., 2005). Not only the type of bacteria but also the source and concentration of the active plant extract compounds and the film composition play a key role in the antimicrobial activity of OEO. For instance, whey protein isolated (WPI)-

Table 5
Antibacterial activity against *Staphylococcus aureus* of the compression-molded sheets made of poly(3-hydroxybutyrate-*co*-3-hydroxyvalerate) (PHBV) and coconut fibers (CFs) loaded with oregano essential oil (OEO).

Sample	Initial		After 15 days	
	Bacterial counts [log (CFU/ml)]	R	Bacterial counts [log (CFU/ml)]	R
Inoculation	5.69 ± 0.10	–	5.69 ± 0.10	–
Control (t = 0 h)	5.70 ± 0.03	–	5.68 ± 0.44	–
Control (t = 24 h)	5.69 ± 0.03	–	5.68 ± 0.44	–
PHBV	5.32 ± 0.50	0.37 ± 0.49	5.30 ± 0.05	0.38 ± 0.41
PHBV/CFs 1 wt.-%	5.48 ± 0.18	0.21 ± 0.15	5.42 ± 0.51	0.26 ± 0.65
PHBV/CFs 1 wt.-% + OEO	4.72 ± 0.05	0.97 ± 0.18	5.56 ± 0.17	0.12 ± 0.29
PHBV/CFs 3 wt.-%	5.39 ± 1.11	0.30 ± 1.14	5.54 ± 0.56	0.14 ± 0.47
PHBV/CFs 3 wt.-% + OEO	4.21 ± 0.50	1.48 ± 0.64	4.78 ± 0.09	0.90 ± 0.65
PHBV/CFs 5 wt.-%	5.36 ± 0.50	0.33 ± 0.51	5.62 ± 0.05	0.06 ± 0.45
PHBV/CFs 5 wt.-% + OEO	4.15 ± 0.70	1.54 ± 0.53	4.58 ± 0.09	1.10 ± 0.12
PHBV/CFs 10 wt.-%	5.35 ± 0.09	0.34 ± 0.09	5.60 ± 0.16	0.08 ± 0.56
PHBV/CFs 10 wt.-% + OEO	3.96 ± 0.33	1.73 ± 0.40	4.32 ± 0.26	1.36 ± 0.41

based films with 1 wt./vol.-% OEO prepared by Oussalah et al. (2004) were effective against different bacterial colonies on the surface of beef. However, Seydim and Sarikus (2006) observed that a content of at least 2 wt.-% OEO in WPI films was needed to reach the minimum inhibitory level against the same bacteria.

Finally, Table 5 includes the antibacterial effect against *S. aureus* of the green composite sheets with varying functionalized CF contents. It can be observed that both the unfilled PHBV sheet and the different green composite sheets containing CFs without OEO showed no inhibition effect on the bacterial growth ($R \leq 0.5$). In contrast, the incorporation of OEO-containing CFs into the PHVB sheets exhibited a significant antibacterial activity. At the initial day, *i.e.* for the tests carried out 1 day after production of the green composite sheets, bacterial reduction on the sheets surface gradually increased with the OEO-containing CFs content. At the lowest content, *i.e.* 1 wt.-% OEO-containing CFs, the green composite sheet presented a slight antibacterial activity ($R = 0.97$). For higher contents, *i.e.* 3–10 wt.-% OEO-containing CFs, the sheets generated a significant surface reduction ($R \geq 1$ and < 3). Although none of the sheets produced a strong reduction ($R \geq 3$), contents as low as 3 wt.-% OEO-containing CFs successfully inhibited the bacterial growth. Indeed, materials with surface reduction values in the range 1–2 are usually considered as bacteriostatic (Fabra, Pourrahimi, Olsson, & Lagaron, 2017). Therefore, final OEO contents of only 0.15 wt.-% in the green composites, which corresponds to a OEO-containing CFs loading of 3 wt.-%, were able to provide a bacteriostatic effect against *S. aureus*. As also shown in the table, after 15 days, the green composite sheets successfully kept a significant antibacterial activity. In particular, the sheets with OEO-containing CFs loadings of 5 and 10 wt.-% still presented significant ($R \geq 1$ and < 3) values of reduction while these presented slight ($R \geq 0.5$ and < 1) and non-significant ($R \leq 0.5$) values for loadings of 3 and 1 wt.-%, respectively. This suggests that, though part of OEO was released from the sheets over time, the CFs were still able to retain a significant amount of the active oil.

Previous studies based on films loaded with OEO against food spoilage microorganisms have shown that a minimum concentration of approximately 1 wt.-% of active material was necessary to ensure antibacterial efficacy. For instance, Benavides et al. (2012) incorporated OEO in alginate films prepared by solvent casting where active contents at a level of 1.0 wt./vol.-% provided antibacterial properties. In another study, Hosseini et al. (2015) prepared OEO-containing fish gelatin/chitosan films also by the casting method, showing antimicrobial performance at 1.2 wt./vol.-%. Pelissari et al. (2009) recently produced starch/chitosan films in which OEO was incorporated at 0.1–1 wt.-% by blow film extrusion. The antimicrobial activity against *S. aureus* was only evaluated qualitatively by the disk inhibition zone assay, producing halos between 13.26 and 30.81 mm. The here-attained results then suggest that antimicrobial efficiency of the green composites based on OEO-containing CFs is about 6–7 times higher than that observed in previous research works. However, all these studies are certainly difficult to compare in a straight way, even for the same bacteria, due to differences in the film nature, the selected methodology of film preparation, the performed antimicrobial test, *etc.*

4. Conclusions

The first part of the present study was focused on finding the right processing conditions to optimally prepare green composites made of PHBV and CFs. Incorporation of different weight contents of CFs into a PHBV matrix was successfully achieved by TSE, varying the screw speed, and afterward shaped into sheets by compression molding. Optimal incorporation of the CFs into the PHBV matrix was attained at 150 rpm since this provided the best balance between dispersion and fiber attrition. This processing condition led to easily processable green composite formulations with the most balanced fiber distribution, average fiber length, and intermediate residence times. In particular, the fibers aspect ratio varied from 5.5 to 9, which decreased with increasing the CF content, and the residence time was of the order of 100 s. It was considered that this processing condition is beneficial to process both PHBV, due to its intrinsic narrow processing window and poor melt strength, and OEO, which is thermolabile and easily evaporates and/or decomposes during processing. In the second part of the study, the green composite sheets prepared at 150 rpm were fully characterized in terms of their thermal, mechanical, and barrier properties. Results showed that the incorporation of CFs into PHBV generated green composite sheets with similar thermal stability, even at the highest content, thus positively not impairing its processing window. In general, the green composites presented a slightly higher rigidity but lower ductility. It was particularly observed that the CFs acted as an effective reinforcement in the PHBV matrix when their length exceeds a critical threshold of 1500 μm, which corresponds to an aspect ratio close to 7. In relation to the barrier properties, it was observed that both the WVP and LP values were slightly reduced due to the CFs presence, which was related to a sorption phenomenon at the filler–matrix interface. Interestingly, the oxygen barrier performance was improved for intermediate CFs contents due to the contribution of the blocking effect over the heterogeneities was optimal. Finally, in the third part of the study, the CFs were impregnated with different OEO contents by an in-house developed spraying methodology and thereafter incorporated again into the green composites to generate sheets with antibacterial activity. Through this approach, it was possible to successfully achieve bacteriostatic effect against *S. aureus* from OEO-containing CF contents of only 3 wt.-%. This was ascribed to the high capacity of CFs to entrap active substances, being able to resist typical processing conditions of thermoplastic materials produced in the packaging industry. Interestingly, OEO was released in a slow manner to the green composite sheet surface, remaining at effective concentrations for a period of at least 15 days.

The scientific merit of this work relays on the development of a fully bio-based formulation, where a natural antimicrobial is incorporated within the structure of an agro-food waste filler, which then acts as a carrier. In addition, the filler also serves to improve the physical performance and potentially reduce the cost of the overall formulation giving the current high price of commercial PHBV. This technology adds to actual strategies to pursue Circular Economy's approaches for the design of packaging materials. The active antimicrobial performance is, indeed, an added value also for the formulation because it will potentially increase the food quality and safety of the packed foods.

Acknowledgements

This research was funded by the EU H2020 project YPACK (reference number 773872), the Spanish Ministry of Economy and Competitiveness (MINECO) project AGL2015-63855-C2-1-R, the Portuguese Foundation for Science and Technology (FCT) under the scope of the strategic funding of UID/BIO/04469/2013 unit and COMPETE 2020 (POCI-01-0145-FEDER-006684), and the BioTecNorte operation (NORTE-01-0145-FEDER-000004) funded by the European Regional Development Fund (ERDF) under the scope of Norte2020 – Programa Operacional Regional do Norte. Prof. Sergio Torres-Giner wants to thank the European Cooperation in Science and Technology (COST) Action FP1405, ActInPak, for financial support during his Short Term Scientific Mission (STSM) at the University of Minho.

References

Avella, M., Rota, G. L., Martuscelli, E., Raimo, M., Sadocco, P., Elegir, G., & Riva, R. (2000). Poly(3-hydroxybutyrate-co-3-hydroxyvalerate) and wheat straw fibre composites: Thermal, mechanical properties and biodegradation behaviour. *Journal of Materials Science, 35*(4), 829–836.

Barham, P. J., Keller, A., Otun, E. L., & Holmes, P. A. (1984). Crystallization and morphology of a bacterial thermoplastic: Poly-3-hydroxybutyrate. *Journal of Materials Science, 19*(9), 2781–2794.

Barkoula, N. M., Garkhail, S. K., & Peijs, T. (2010). Biodegradable composites based on flax/polyhydroxybutyrate and its copolymer with hydroxyvalerate. *Industrial Crops and Products, 31*(1), 34–42.
Benavides, S., Villalobos-Carvajal, R., & Reyes, J. E. (2012). Physical, mechanical and antibacterial properties of alginate film: Effect of the crosslinking degree and oregano essential oil concentration. *Journal of Food Engineering, 110*(2), 232–239.
Bhatnagar, A., Vilar, V. J. P., Botelho, C. M. S., & Boaventura, R. A. R. (2010). Coconut-based biosorbents for water treatment — A review of the recent literature. *Advances in Colloid and Interface Science, 160*(1), 1–15.
Bogoeva-Gaceva, G., Avella, M., Malinconico, M., Buzarovska, A., Grozdanov, A., Gentile, G., et al. (2007). Natural fiber eco-composites. *Polymer Composites, 28*(1), 98–107.
Bugnicourt, E., Cinelli, P., Lazzeri, A., & Alvarez, V. (2014). Polyhydroxyalkanoate (PHA): Review of synthesis, characteristics, processing and potential applications in packaging. *Express Polymer Letters, 8*(11), 791–808.
Burt, S. (2004). Essential oils: Their antibacterial properties and potential applications in foods—A review. *International Journal of Food Microbiology, 94*(3), 223–253.
Castro-Mayorga, J. L., Fabra, M. J., Pourrahimi, A. M., Olsson, R. T., & Lagaron, J. M. (2017). The impact of zinc oxide particle morphology as an antimicrobial and when incorporated in poly(3-hydroxybutyrate-co-3-hydroxyvalerate) films for food packaging and food contact surfaces applications. *Food and Bioproducts Processing, 101*(Supplement C), 32–44.
Cherpinski, A., Torres-Giner, S., Cabedo, L., Méndez, J. A., & Lagaron, J. M. (2017). Multilayer structures based on annealed electrospun biopolymer coatings of interest in water and aroma barrier fiber-based food packaging applications. *Journal of Applied Polymer Science, 135*(24), 45501.
Choudhury, A., Kumar, S., & Adhikari, B. (2007). Recycled milk pouch and virgin low-density polyethylene/linear low-density polyethylene based coir fiber composites. *Journal of Applied Polymer Science, 106*(2), 775–785.
Corradini, E., de Morais, L. C., Rosa, M. F., Mazzetto, S. E., Mattoso, L. H. C., & Agnelli, J. A. M. (2006). A preliminary study for the use of natural fibers as reinforcement in starch-gluten-glycerol matrix. *Macromolecular Symposia, 245–246*(1), 558–564.
Cunha, M., Berthet, M.-A., Pereira, R., Covas, J. A., Vicente, A. A., & Hilliou, L. (2015). Development of polyhydroxyalkanoate/beer spent grain fibers composites for film blowing applications. *Polymer Composites, 36*(10), 1859–1865.
Dadalioğlu, I., & Evrendilek, G. A. (2004). Chemical compositions and antibacterial effects of essential oils of Turkish oregano (Origanum minutiflorum), Bay laurel (Laurus nobilis), Spanish Lavender (Lavandula stoechas L.), And fennel (Foeniculum vulgare) on Common foodborne pathogens. *Journal of Agricultural and Food Chemistry, 52*(26), 8255–8260.
dos Santos Rodrigues, J. B., de Carvalho, R. J., de Souza, N. T., de Sousa Oliveira, K., Franco, O. L., Schaffner, D., de Souza, E. L., et al. (2017). Effects of oregano essential oil and carvacrol on biofilms of Staphylococcus aureus from food-contact surfaces. *Food Control, 73*(Part B), 1237–1246.
Faruk, O., Bledzki, A. K., Fink, H.-P., & Sain, M. (2014). Progress report on natural fiber reinforced composites. *Macromolecular Materials and Engineering, 299*(1), 9–26.
Geethamma, V. G., Thomas Mathew, K., Lakshminarayanan, R., & Thomas, S. (1998). Composite of short coir fibres and natural rubber: Effect of chemical modification, loading and orientation of fibre. *Polymer, 39*(6), 1483–1491.
Gu, H. (2009). Tensile behaviours of the coir fibre and related composites after NaOH treatment. *Materials & Design, 30*(9), 3931–3934.
Hasan, M., Hoque, M. E., Mir, S. S., Saba, N., & Sapuan, S. M. (2015). Manufacturing of coir fibre-reinforced polymer composites by Hot compression technique. In M. S. Salit, M. Jawaid, N. B. Yusoff, & M. E. Hoque (Eds.). *Manufacturing of natural fibre reinforced polymer composites* (pp. 309–330). Cham: Springer International Publishing.
Hilliou, L., Teixeira, P. F., Machado, D., Covas, J. A., Oliveira, C. S. S., Duque, A. F., et al. (2016). Effects of fermentation residues on the melt processability and thermo-mechanical degradation of PHBV produced from cheese whey using mixed microbial cultures. *Polymer Degradation and Stability, 128*(Supplement C), 269–277.
Hosseini, S. F., Rezaei, M., Zandi, M., & Farahmandghavi, F. (2015). Bio-based composite edible films containing Origanum vulgare L. essential oil. *Industrial Crops and Products, 67*, 403–413.
Hosseini, S. F., Zandi, M., Rezaei, M., & Farahmandghavi, F. (2013). Two-step method for encapsulation of oregano essential oil in chitosan nanoparticles: Preparation, characterization and in vitro release study. *Carbohydrate Polymers, 95*(1), 50–56.
Joshi, S. V., Drzal, L. T., Mohanty, A. K., & Arora, S. (2004). Are natural fiber composites environmentally superior to glass fiber reinforced composites? *Composites Part A: Applied Science and Manufacturing, 35*(3), 371–376.
Kunioka, M., Tamaki, A., & Doi, Y. (1989). Crystalline and thermal properties of bacterial copolyesters: Poly(3-hydroxybutyrate-co-3-hydroxyvalerate) and Poly(3-hydroxybutyrate-co-4-hydroxybutyrate). *Macromolecules, 22*(2), 694–697.
Lagaron, J. M. (2011). *1 - Multifunctional and nanoreinforced polymers for food packaging. Multifunctional and nanoreinforced polymers for food packaging*. Cambridge, UK: Woodhead Publishing1–28.
López, P., Sánchez, C., Batlle, R., & Nerín, C. (2007). Development of flexible antimicrobial films using essential oils as active agents. *Journal of Agricultural and Food Chemistry, 55*(21), 8814–8824.
Mir, S. S., Nafsin, N., Hasan, M., Hasan, N., & Hassan, A. (2013). Improvement of physico-mechanical properties of coir-polypropylene biocomposites by fiber chemical treatment. *Materials & Design (1980–2015), 52*(Supplement C), 251–257.
Oussalah, M., Caillet, S., Salmiéri, S., Saucier, L., & Lacroix, M. (2004). Antimicrobial and antioxidant effects of milk protein-based film containing essential oils for the preservation of whole beef muscle. *Journal of Agricultural and Food Chemistry, 52*(18), 5598–5605.
Owolabi, O., & Czvikovszky, T. (1988). Composite materials of radiation-treated coconut fiber and thermoplastics. *Journal of Applied Polymer Science, 35*(3), 573–582.
Pelissari, F. M., Grossmann, M. V. E., Yamashita, F., & Pineda, E. A. G. (2009). Antimicrobial, mechanical, and barrier properties of cassava starch – chitosan films incorporated with oregano essential oil. *Journal of Agricultural and Food Chemistry, 57*(16), 7499–7504.
Razumovskii, L. P., Iordanskii, A. L., Zaikov, G. E., Zagreba, E. D., & McNeill, I. C. (1994). Sorption and diffusion of water and organic solvents in poly(β-hydroxybutyrate) films. *Polymer Degradation and Stability, 44*(2), 171–175.
Rosa, M. F., Chiou, B.-s., Medeiros, E. S., Wood, D. F., Williams, T. G., Mattoso, L. H. C., et al. (2009). Effect of fiber treatments on tensile and thermal properties of starch/ethylene vinyl alcohol copolymers/coir biocomposites. *Bioresource Technology, 100*(21), 5196–5202.
Rosa, M. F., Medeiros, E. S., Malmonge, J. A., Gregorski, K. S., Wood, D. F., Mattoso, L. H. C., et al. (2010). Cellulose nanowhiskers from coconut husk fibers: Effect of preparation conditions on their thermal and morphological behavior. *Carbohydrate Polymers, 81*(1), 83–92.
Sanchez-Garcia, M. D., Gimenez, E., & Lagaron, J. M. (2007). Novel PET nanocomposites of interest in food packaging applications and comparative barrier performance with biopolyester nanocomposites. *Journal of Plastic Film & Sheeting, 23*(2), 133–148.
Sanchez-Garcia, M. D., Gimenez, E., & Lagaron, J. M. (2008). Morphology and barrier properties of solvent cast composites of thermoplastic biopolymers and purified cellulose fibers. *Carbohydrate Polymers, 71*(2), 235–244.
Satyanarayana, K. G., Pillai, C. K. S., Sukumaran, K., Pillai, S. G. K., Rohatgi, P. K., & Vijayan, K. (1982). Structure property studies of fibres from various parts of the coconut tree. *Journal of Materials Science, 17*(8), 2453–2462.
Seydim, A. C., & Sarikus, G. (2006). Antimicrobial activity of whey protein based edible films incorporated with oregano, rosemary and garlic essential oils. *Food Research International, 39*(5), 639–644.
Shang, L., Fei, Q., Zhang, Y. H., Wang, X. Z., Fan, D.-D., & Chang, H. N. (2012). Thermal properties and biodegradability studies of poly(3-hydroxybutyrate-co-3-hydroxyvalerate). *Journal of Polymers and the Environment, 20*(1), 23–28.
Shibata, M., Oyamada, S., Kobayashi, S., & Yaginuma, D. (2004). Mechanical composites and biodegragability of green composites based on biodegradable polyesters and lyocell fabric. *Journal of Applied Polymer Science, 92*(6), 3857–3863.
Teramoto, N., Urata, K., Ozawa, K., & Shibata, M. (2004). Biodegradation of aliphatic polyester composites reinforced by abaca fiber. *Polymer Degradation and Stability, 86*(3), 401–409.
Tomczak, F., Sydenstricker, T. H. D., & Satyanarayana, K. G. (2007). Studies on lignocellulosic fibers of Brazil. Part II: Morphology and properties of Brazilian coconut fibers. *Composites Part A: Applied Science and Manufacturing, 38*(7), 1710–1721.
Torres-Giner, S. (2016). *Preparation of conductive carbon black-filled polymer nanocomposites via melt compounding. Conductive Materials and Composites*. New York, US: Nova Science Publishers, Inc117–164.
Torres-Giner, S., Montanes, N., Boronat, T., Quiles-Carrillo, L., & Balart, R. (2016). Melt grafting of sepiolite nanoclay onto poly(3-hydroxybutyrate-co-4-hydroxybutyrate) by reactive extrusion with multi-functional epoxy-based styrene-acrylic oligomer. *European Polymer Journal, 84*(Supplement C), 693–707.
Torres-Giner, S., Montanes, N., Fombuena, V., Boronat, T., & Sanchez-Nacher, L. (2016). Preparation and characterization of compression-molded green composite sheets made of poly(3-hydroxybutyrate) reinforced with long pita fibers. *Advances in Polymer Technology*. http://dx.doi.org/10.1002/adv.21789.
Torres-Giner, S., Torres, A., Ferrándiz, M., Fombuena, V., & Balart, R. (2017). Antimicrobial activity of metal cation-exchanged zeolites and their evaluation on injection-molded pieces of bio-based high-density polyethylene. *Journal of Food Safety, 37*(4), e12348.
Wambua, P., Ivens, J., & Verpoest, I. (2003). Natural fibres: Can they replace glass in fibre reinforced plastics? *Composites Science and Technology, 63*(9), 1259–1264.
Westerlind, B. S., & Berg, J. C. (1988). Surface energy of untreated and surface-modified cellulose fibers. *Journal of Applied Polymer Science, 36*(3), 523–534.
Yang, H.-S., Kim, H.-J., Park, H.-J., Lee, B.-J., & Hwang, T.-S. (2006). Water absorption behavior and mechanical properties of lignocellulosic filler–polyolefin bio-composites. *Composite Structures, 72*(4), 429–437.
Zini, E., & Scandola, M. (2011). Green composites: An overview. *Polymer Composites, 32*(12), 1905–1915.
Zivanovic, S., Chi, S., & Draughon, A. F. (2005). Antimicrobial activity of chitosan films enriched with essential oils. *Journal of Food Science, 70*(1), M45–M51.